

# ARNT-Deficient Mice and Placental Differentiation

Katherine R. Kozak, Barbara Abbott,\* and Oliver Hankinson<sup>1</sup>

Department of Pathology and Laboratory Medicine, Jonsson Comprehensive Cancer Center, and Molecular Biology Institute, University of California Los Angeles, California 90095-1732; and \*Reproductive Toxicology Division, National Health and Environmental Effects Research Laboratory, U.S. Environmental Protection Agency, Research Triangle Park, North Carolina 27711

**We used homologous recombination in embryonic stem cells to generate mice heterozygous for an aryl hydrocarbon nuclear translocator (ARNT) null mutation. These mice were intercrossed, but no live homozygous *Arnt*  $-/-$  knockout mice were produced among 64 newborns. Homozygotes die *in utero* between 9.5 and 10.5 days of gestation. Abnormalities included neural tube closure defects, forebrain hypoplasia, delayed rotation of the embryo, placental hemorrhaging, and visceral arch abnormalities. However, the primary cause of lethality appears to be failure of the embryonic component of the placenta to vascularize and form the labyrinthine spongiotrophoblast. This may be related to ARNT's known role in hypoxic induction of angiogenesis. We found no defects in yolk sac circulation. © 1997 Academic Press**

## INTRODUCTION

The aryl hydrocarbon nuclear translocator protein (ARNT) is a founding member of the basic helix-loop-helix/Per-ARNT-Sim (bHLH/PAS) family of transcription factors. The basic motif of these proteins is involved in sequence-dependent recognition of DNA, while the PAS domain acts in concert with the bHLH domain to form a dimerization surface (Reisz-Porszasz *et al.*, 1994; Fukunaga *et al.*, 1995). We and others have demonstrated that ARNT interacts with several other members of the bHLH/PAS family. These include the aryl hydrocarbon receptor, which after binding ligand dimerizes with ARNT and activates transcription of a number of target genes, including *CYP1A1*, the products of which are involved in the metabolism of aryl hydrocarbons to toxic or carcinogenic intermediates (reviewed by Hankinson, 1995); SIM-1 (single-minded 1) and SIM-2, which may be involved in developmental regulation of the mouse central nervous system (Ema *et al.*, 1996; Probst *et al.*, 1997); hypoxia-inducible factor 1 $\alpha$  (HIF-

1 $\alpha$ ), which as a dimer with ARNT is involved in mediating cellular responses to hypoxia (Wang and Semenza, 1995) including increased expression of vascular endothelial growth factor (VEGF; Wood *et al.*, 1996); and endothelial PAS domain protein 1 (EPAS1/HLF), which appears to be a regulator of embryonic vascularization with activation of EPAS1 being stimulated by hypoxic conditions (Tian *et al.*, 1997; Ema *et al.*, 1997). As a step toward elucidating the physiological function of ARNT in the whole organism, we generated and analyzed *Arnt*-deficient transgenic mice.

## MATERIALS AND METHODS

### Generation of Mice Heterozygous for an *Arnt* Null Allele

A genomic library developed from the 129/SvJ mouse strain (Stratagene) was probed with a PCR-amplified (650 bp) fragment of mouse *Arnt* cDNA encompassing the bHLH domain, and a 6-kb *Arnt* genomic fragment was isolated. The segment of the mouse *Arnt* gene encoding the bHLH region is contained within a single exon, corresponding to amino acids 92 to 162. A targeting plasmid was constructed (Fig. 1A) that included the 6-kb *Arnt* fragment with the bHLH domain interrupted by insertion of a neomycin phosphotransferase cassette (pMC1 $neopA$ ; Thomas and Capecchi, 1987), and flanked on either side by a herpes simplex thymidine

<sup>1</sup> To whom correspondence should be addressed at Department of Pathology and Laboratory Medicine, University of California, Los Angeles Medical Center, Center for the Health Sciences, Los Angeles, CA 90095-1732. Fax: (310) 794-9272; E-mail: ohank@pathology.medsch.ucla.edu.

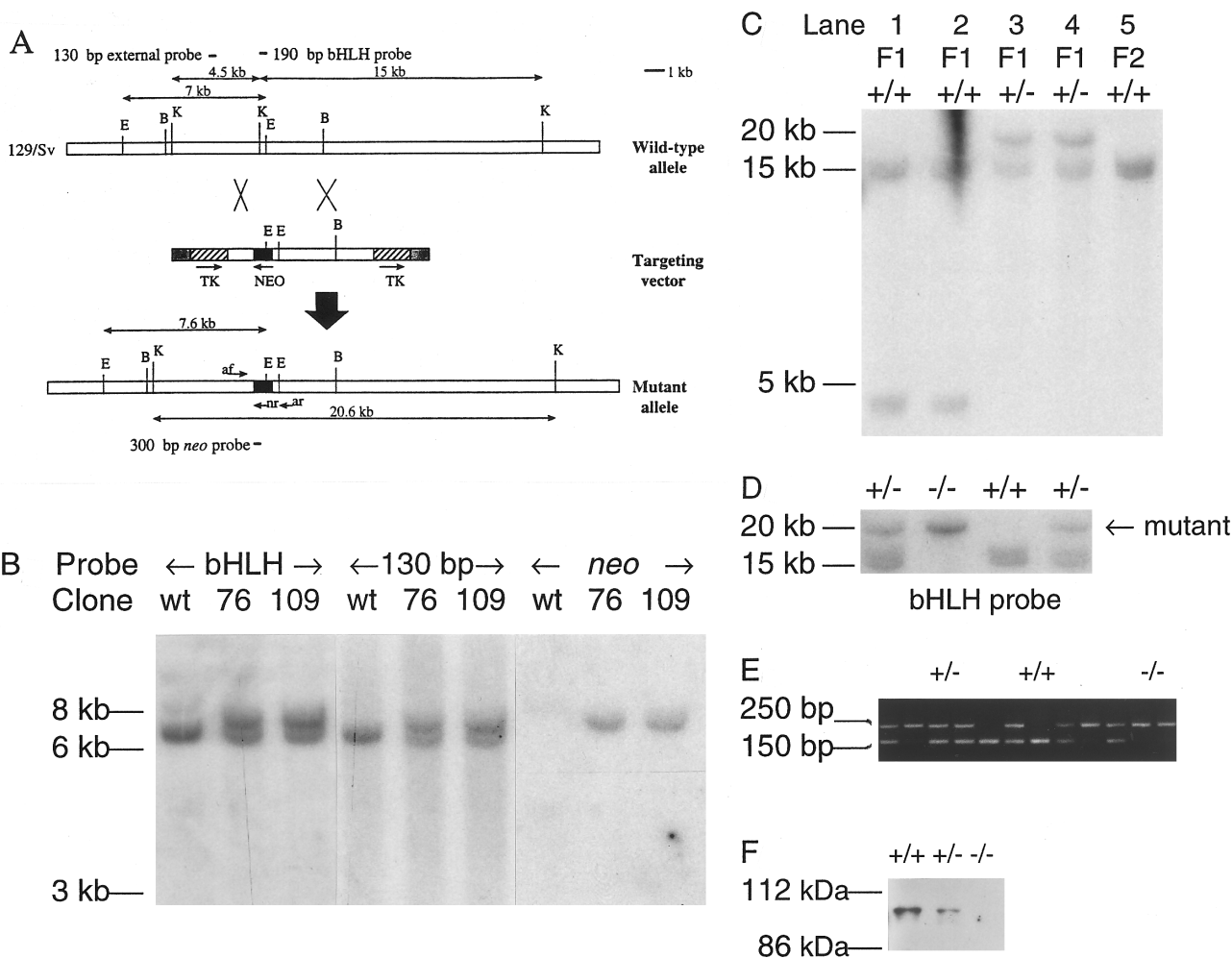


**FIG. 1.** (A) Targeting strategy. The wild-type allele, the targeting vector and the mutant allele are shown. The pMC1-neomycin resistance cassette and pMC1-thymidine kinase cassette are designated as NEO and TK, respectively. Arrows show the orientation of the genes. Restriction enzyme sites used for cloning and Southern blot analysis are indicated (B, *Bst*EII; E, *Eco*RI; K, *Kpn*I). The double-arrow lines indicate the sizes of restriction fragments hybridizing to the probes used for Southern blot analysis. (B) Southern blot analysis of *Eco*RI-digested genomic DNA prepared from neomycin- and FIAU-resistant ES cell clones hybridized to the probes indicated in A (data for clones 76 and 109 shown). The size for the *Eco*RI fragment associated with the ES cell wild-type allele hybridized with either the bHLH or 130-bp probe is 7 kb, while no fragment is identified with the *neo* probe. The targeted allele, due to insertion of 1.1 kb and addition of an *Eco*RI site, resulted in *Eco*RI fragments of 7.6 kb for all probes (a faint 0.6-kb fragment was also observed with the bHLH probe, as expected). Proper insertion was also demonstrated by digestion with *Bst*EII and *Kpn*I (data not shown). No additional hybridization bands were observed in clone 76 or 109, indicating that there were no nonhomologous insertions. Clones 76 and 109, isolated from independent electroporations, were used to generate chimeric mice which were then mated to C57BL/6J females. (C) Identification of heterozygous progeny. Tail DNA of light chinchilla offspring from male chimeras derived from clone 109 mated with C57BL/6J females were digested with *Kpn*I and hybridized to the bHLH probe. In +/+ light chinchilla progeny, the bHLH probe recognized ES cell (129/SvJ) wild-type genomic DNA fragments of 4.5 and 15 kb and C57BL/6J wild-type genomic DNA fragments of 15 and 16.5 kb. In +/- light chinchilla progeny, the bHLH probe recognized C57BL/6J wild-type genomic DNA fragments of 15 and 16.5 kb and an ES cell-derived (129/SvJ) targeted fragment of 20.6 kb. The size difference of the wild-type bands is due to polymorphism between 129/Sv and C57BL/6. (D) Southern blot analysis of *Kpn*I-digested DNA isolated from embryo or yolk sac derived from progeny of heterozygous intercrosses probed with the bHLH probe. (E) PCR analysis of individual, day 9.5 embryonic DNA isolated from progeny of heterozygous intercrosses with one forward and two reverse primers used simultaneously (af, ar, nr) to detect the targeted *Arnt* allele and the wild-type *Arnt* allele. The *Arnt* forward and reverse pair amplifies a 150-bp wild-type band and the *Arnt* forward and *neo* reverse pair amplifies a 250-bp recombinant band. (F) Western blot analysis of ARNT expression. Western blot analysis was performed using affinity-purified rabbit-ARNT antiserum directed against the carboxy terminus half of the ARNT protein as described previously (Probst *et al.*, 1993) and developed using the SuperSignal ULTRA chemiluminescent substrate (Pierce). Extracts (~50  $\mu$ g of protein) from embryonic tissue isolated from +/+, +/-, and -/- GD 9.5 embryos were applied on 7.5% SDS-PAGE.

kinase (HSV-*tk*) expression cassette (pMC1*tk* pA). The *neo* cassette was inserted into a unique *KpnI* site in the *Arnt* DNA fragment giving rise to one *Arnt* arm of approximately 1.3 kb and the other of about 4.7 kb. The *KpnI* site was destroyed in the ligation and an *EcoRI* site was introduced. The transcriptional orientation of the neomycin-resistance gene was opposite to that of the *Arnt* gene. A null mutation was expected because the reverse orientation of the *neo* cassette contains multiple stop codons in each reading frame. If exon skipping did occur, it would delete the bHLH domain required for dimerization and DNA binding and any resultant protein would be nonfunctional.

The targeting vector was linearized at a unique *HindIII* site in the bacterial backbone and electroporated into 129/SvJ germline competent RW4 ES cells (Genome Systems). Electroporated embryonic stem (ES) cells were plated onto a monolayer of  $\gamma$ -irradiated, neomycin-resistant mouse primary fibroblasts and were grown in the presence of LIF (1000 u/ml, GIBCO-BRL). Putative homologous recombinants were identified by selection of resistant colonies in 250  $\mu$ g/ml G418 (geneticin; GIBCO-BRL) and 0.2  $\mu$ M FIAU (1-[2-deoxy, 2-fluoro- $\beta$ -D-arabinofuranosyl]-5-iodouracil), added after 24 h, and maintained for 10 days (positive-negative selection, Mansour *et al.*, 1988). To confirm single integration events and homologous recombination of the targeting construct, each clone was analyzed by Southern blot of genomic DNA using the following probes: (1) a 190-bp bHLH-specific probe spanning the disrupted *KpnI* site, (2) a 130-bp *Arnt*-specific probe external to the region found in the construct, identifying only true homologous recombination events, and (3) a 300-bp *neo*-specific probe identifying all integration events, including random events (Fig. 1B).

Two correctly targeted 129/SvJ ES cells were microinjected into C57BL/6J blastocysts isolated at day 3.5 (Bradley, 1987). The blastocysts were introduced into pseudopregnant females and chimeric males among the resulting progeny were mated to C57BL/6J females. Light chinchilla progeny were genotyped and *Arnt* heterozygosity identified by Southern analysis of tail DNA. Mice heterozygous for the targeted mutation were then intercrossed to obtain mice homozygous for the disrupted *Arnt* null allele.

### Genotyping Mice and Embryos

Genotyping of adult mice was performed by Southern blot analysis of digested tail DNA. The genotypes of dissected embryos were determined by Southern blot analysis or PCR using DNA isolated from yolk sac or embryo. The PCR primers corresponded to the bHLH domain (*Arnt* forward [af], 5'-CATAGTGAAATAGAACGG-CGGCG-3'; *Arnt* reverse [ar], 5'-AGGACTTCATGTGAGAAA-CGGC-3') and the *neo* gene (*neo* reverse [nr], 5'-TGGCGGCGA-ATGGGCTGACC-3').

### Analysis of Embryos

Embryos were harvested from matings between heterozygotes for the *Arnt* mutation between gestation day (GD) 7.5 and 17.5. Expression of ARNT was determined in the GD 9.5 conceptus by immunostaining (Abbott and Probst, 1995). Sections of all three genotypes (+/+, +/-, -/-) were processed on a single slide. Vasculogenesis and angiogenesis were assessed by PECAM immunostaining of endothelial cells using a purified anti-mouse CD31 (PharMingen; San Diego, CA; diluted 1:1000) and detected with biotin conjugated anti-rat AffiniPure antibody (Jackson Immunoresearch Laboratories, West Grove, PA) and the Vector ABC Kit for peroxi-

dase (Vector Labs, Burlingame, CA). Feulgen stain of the yolk sac was performed by microinjecting Feulgen into the chorionic space immediately after collection of the conceptus, before opening the extraembryonic membranes. Embryos of similar developmental stages as determined by somite numbers were chosen for our comparison studies in order to rule out any differences resulting from developmental delay or arrest (e.g., developmentally retarded embryos may have immature yolk sacs and placenta).

A simple regression model was used to compare dead/resorbed or developmentally delayed/abnormal embryos to gestation day. For statistical analysis of somite number and embryo size within a gestation day, an analysis of variance was performed. A mixed effects linear model was used to associate size with somite number between genotypes. A Pearson  $\chi^2$  analysis was performed on genotype ratios.

## RESULTS

### Generation of Mice Heterozygous for an *Arnt* Null Mutation

An *Arnt*-targeting vector was transfected into ES cells and putative homologous recombinants isolated by selection in geneticin (G418) and FIAU. Southern blot analysis of 131 clones detected 3 in which one *Arnt* allele was disrupted by homologous recombination and in which no other plasmid integration events had occurred (Figs. 1A and 1B). Two clones were injected into C57BL/6J blastocysts and chimeric mice were generated. Both clones gave several male chimeras with ES coat color contribution greater than 80%. Light chinchilla progeny (F1) were genotyped by Southern analysis of tail DNA (Fig. 1C). Only clone 109 transmitted the ES cells through the germline when chimeras were mated with C57BL/6J females. Of the five male chimeras generated from clone 109, three of them transmitted the mutant allele to offspring, yielding *Arnt* (+/-) heterozygotes.

### Lethality of *Arnt* -/- Mice in Utero

Mice heterozygous for the targeted mutation were intercrossed, but no live homozygous *Arnt* -/- mice were produced among 64 neonates from 14 litters. Pregnant females from *Arnt* +/- intercrosses were sacrificed at different times of gestation, and -/- mutants were identified by Southern blotting (Fig. 1D) and/or PCR (Fig. 1E). Results demonstrated that most homozygous embryos die between GD 9.5 and 10.5. The distribution of genotypes in GD 8.5 to 10.5 embryos (dead or alive) from 17 heterozygous matings was 32:70:24 (+/+, +/-, and -/-, respectively) and is not statistically different from the expected ratio of 1:2:1. From GD 11.5 to 17.5 and postnatally, all viable pups were either +/+ or +/- (36 and 59, respectively) and this distribution does not differ significantly from a 1:2 ratio. Thus no evidence for embryonic lethality of the *Arnt* +/- heterozygote was obtained.

### Expression of ARNT in the Conceptus

ARNT protein expression in the embryos was analyzed by Western blotting (Fig. 1F). The level of ARNT was approximately twofold greater in  $+/+$  embryos than in  $+/-$  embryos and was undetectable in  $-/-$  embryos (Fig. 1E). Extensive expression of ARNT was detectable by immunohistochemical analysis throughout the GD 9.5 *Arnt*  $+/+$  and *Arnt*  $+/-$  embryos, while no expression was detectable in *Arnt*  $-/-$  embryos (data not shown). The knockout conceptus also showed no expression of ARNT protein in the placental cells derived from the embryo, although adjacent maternal decidual cells express ARNT (Figs. 2B and 2F). In the  $+/+$  and  $+/-$  placenta, ARNT is expressed in nuclei of the maternal decidual cells, in embryonic trophoblasts, and in the single layer of trophoblast giant cells which surrounds the embryo and lies between the maternal and embryonic placental regions (Figs. 2A and 2E).

### Developmental Delay and Growth Retardation in $-/-$ Embryos

On GD 8.5 the  $-/-$  embryos were not distinguishable from littermates by developmental stage as indicated by somite number (Table 1). Observation of heartbeat and blood circulation in the yolk sac vasculature and in the embryo indicated that GD 8.5 embryos were viable and that vasculogenesis was proceeding normally in  $+/-$  and  $-/-$  embryos. On GD 9.5, the  $-/-$  embryos were at a developmental stage similar to that of  $+/+$  embryos because there was no significant difference in somite numbers (Table 1), but most knockout embryos were growth retarded as indicated by significant decreases in crown rump and head length. By GD 10.5, the embryos were developmentally delayed with significantly decreased somite number. The number of  $-/-$  embryos showing an abnormal phenotype and/or developmental delay was 60% at GD 9.5 and 100% by GD 10.5. Among 15  $-/-$  embryos from 10 litters at GD 9.5, 20% showed delayed rotation, 40% showed placental hemorrhaging, and 40% showed unfused head folds. The severity of neural tube defects ranged from open anterior or posterior neuropore, small open region in the mid- or hindbrain, to complete failure of the head folds to close (Figs. 4A and 4B). We also observed forebrain hypoplasia

which was associated with visceral arch abnormalities, as reflected in decreased head length for  $-/-$  embryos (Table 1).

### Defective Placental Vascolarization in $-/-$ Mice

At GD 9–9.5 the embryonic portion of the placenta forms a primitive allantoic vasculature, while the maternal decidua develops numerous blood-filled clefts. It is at this time that the endothelial cell-lined allantoic cavities contain nucleated embryonic blood cells and the primitive placenta begins to supply nutrients and oxygen to the embryo. We therefore examined vascularization of the placenta by immunostaining with antibody to platelet endothelial cell adhesion molecule (PECAM; Figs. 2C and 2D). In *Arnt* knockout embryos the allantois extends across the exocoelomic cavity and fuses with the chorionic plate. However, the subsequent formation of an extensive endothelial cell-lined vascular network was not observed (Fig. 2D). In contrast, the  $+/+$  and  $+/-$  placenta do not differ morphologically from each other and both form the labyrinth and spongiotrophoblastic layers with abundant endothelial cell-lined vascular networks (Fig. 2C;  $+/-$  data not shown). Thus, the embryonic component of the placenta of the  $-/-$  conceptus was small with fewer PECAM-stained endothelial cell-lined cavities than with the  $+/+$  or  $+/-$  conceptuses. Upon examination of gross morphology, all  $-/-$  GD 9.5 placentas had small chorioallantoic plates in combination with fewer labyrinthine cavities, indicating that the placental region is not differentiating as expected.

Observation of yolk sacs at dissection revealed that an extensive vascular plexus forms and that circulation exists in the major vessels of all genotypes. In sections, the development of the yolk sac in the knockout embryos was similar to that observed for the  $+/+$  embryos. The yolk sacs of all genotypes were vascularized with blood cells in the vessels (Figs. 3A–3G). Vascularization of the yolk sac was also examined in whole-mount Feulgen-stained preparations, and  $-/-$  yolk sac (Figs. 3E and 3G) showed major vessels as well as the fine vessel mesh present in the  $+/-$  (Fig. 3F) and  $+/+$  tissue (data not shown). PECAM staining (Figs. 3C and 3D) showed endothelial cell-lined blood vessels for both  $+/+$  and  $-/-$  embryonic yolk sacs. The separation of adjacent

**FIG. 2.** (A–F) Placenta of GD 9.5 conceptus. (A,B) Expression of ARNT protein. (A) The placenta of the  $+/+$  conceptus showed expression of ARNT in maternal and embryonic compartments and was in the process of vascularization in the spongiotrophoblast and chorioallantoic regions. (B) In contrast, the placenta of the  $-/-$  conceptus was small with minimal vascularization and ARNT was not expressed in the embryonic region. (A and B lightly counterstained with hematoxylin). (C,D) Formation of the chorionic labyrinth and spongiotrophoblastic layer revealed through PECAM staining of endothelial cells. (C) PECAM staining demonstrated the complexity of the vascular network of endothelial-cell lined cavities (arrows) in the  $+/+$  placenta. (D) The  $-/-$  placenta exhibited a few large endothelial-cell-lined cavities (arrows). (E,F) ARNT expression at the maternal–fetal border. (E) ARNT was expressed in maternal and embryonic tissues in the  $+/+$  conceptus with trophoblast giant cells having high levels. (F) ARNT expression was observed in the maternal decidua (d) of the  $-/-$  conceptus; however, in the cells of embryonic origin, including the trophoblast giant cells, ARNT expression was eliminated by the gene knockout. (Bar, 100  $\mu$ m; b, endogenous peroxidase in blood cells; c, chorionic plate; d, maternal decidual placenta; e, embryonic placental tissue; g, trophoblast giant cells; s, spongiotrophoblast; y, yolk sac).

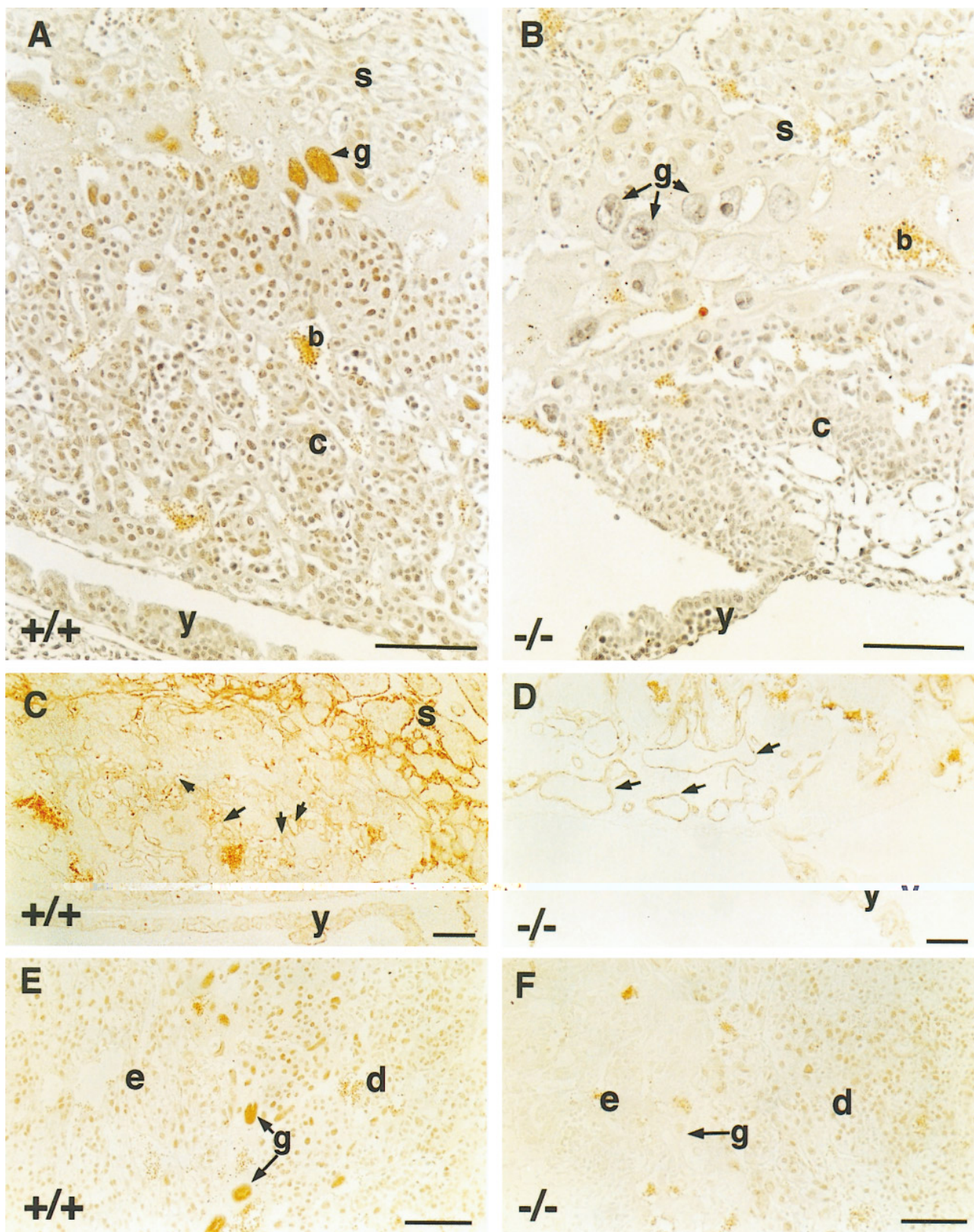


**TABLE 1**  
Effects of Genotype on Growth and Development

		Gestation day		
		8.5	9.5	10.5
<i>n</i> , somites	+/+	6.7 ± 0.9	17.2 ± 1.5	33.8 ± 2.9
	+/-	9.3 ± 0.5	21.0 ± 1.2*	26.9 ± 1.1
	-/-	6.3 ± 1.5	16.7 ± 2.0†	16.0 ± 4.0*†
Crown	+/+	ND	3.1 ± 0.2 <sup>a</sup>	4.9 ± 0.4
Rump	+/-	ND	3.1 ± 0.1 <sup>a</sup>	3.9 ± 0.3
Length (mm)	-/-	ND	2.0 ± 0.2 <sup>a,*†</sup>	3.3 ± 0.5*†
Head	+/+	ND	1.3 ± 0.1	2.7 ± 0.3
Length (mm)	+/-	ND	1.4 ± 0.1	2.1 ± 0.2
	-/-	ND	1.0 ± 0.1*†	1.6 ± 0.2*†

Note. Data from 4, 10, and 5 litters; GD8.5, 9.5, and 10.5, respectively.

<sup>a</sup> Measured from fixed tissues.

\*  $P < 0.05$  vs +/+; † vs +/-.

vessels in the mesh of microvessels showed a range of completeness in all genotypes. Although definite abnormalities in yolk sac vascularization were not observed in -/- yolk sacs, a more thorough analysis would be required to eliminate the possibility that subtle disruptions in angiogenesis could be present.

Our observations suggest that lethality of the *Arnt* knockout is due to failure of the embryonic component of the placenta to vascularize and form the labyrinthine spongio-trophoblast. Deficiency or absence of this labyrinth would compromise further growth and development and lead to embryonic death.

## DISCUSSION

Our *Arnt* knockout results show that the ARNT protein serves an indispensable function in development. The critical events which affect survival of the embryo at GD 8.5 to 10.5 are the development of the yolk sac and chorioallantoic placental circulations. Establishment of circulation occurs at GD 7–8 for the yolk sac and GD 8.5–9 for the placenta. We have shown that the allantois forms in -/- embryos and makes contact with the chorionic plate and that the yolk sac appears normal. However, differentiation of the placenta fails to progress. Major defects in placental differentiation are incompatible with continued embryonic/fetal growth and development, and loss of -/- embryos could be attributed mainly to this problem. Major malformations were often present in -/- embryos. The defects observed were severe and it would be reasonable to expect gross morphological abnormalities (including exencephaly and anencephaly) if these embryos had survived to birth.

The results we describe here differ from those of another group that recently characterized an *Arnt* knockout mouse

(Maltepe *et al.*, 1997), and who postulated that lethality was due to insufficient vascularization of the yolk sac and solid tissues. The *Arnt* knockout of Maltepe and co-workers was readily distinguished from heterozygous or wild-type littermates on GD 9.5 by an absence of blood-filled yolk sac vessels. Our *Arnt* knockout embryos cannot be distinguished from littermates on this basis because all embryos exhibited equivalent development of the yolk sac circulation (Figs. 3E–3G). In our case, circulation of blood cells was observed in large vitelline vessels and through the vascular capillary mesh in all genotypes on GD 9.5. The GD 9.5 -/- embryos of Maltepe and co-workers were described as “smaller and generally wasted, and development was delayed.” Based on this statement, their embryos are in worse condition on GD 9.5 and appear to be dying somewhat earlier than our embryos. Our *Arnt* -/- embryos on GD 9.5 do not show developmental delay (somite numbers are not significantly different between genotypes) and are not degenerating at that age.

The later death of our *Arnt* -/- embryos correlates with insufficiency of placental function, rather than absence of yolk sac circulation. Other knockouts in which lethality of -/- embryos has been ascribed to placental defects die between GD 10 and 10.5. For example, the mammalian *achaete-scute* homolog-2 -/- embryos die from placental failure at GD 10, apparently due to failure to establish a proper chorioallantoic circulation (Guillemot *et al.*, 1994), while most vascular cell adhesion molecule -/- embryos die between GD 10 and 11, apparently either due to lack of allantoic fusion with the chorion or abnormal distribution of the allantoic mesoderm over the chorionic surface (Gurtner *et al.*, 1995).

Differences in phenotype between our knockouts and those of Maltepe and co-workers may represent defects in the same pathway which manifest at different developmental stages in the two populations of mice. It is conceivable that the differences are attributable to differences in genomic background, although the knockouts from both groups were generated by intercrossing 129/Sv × C57BL/6 parental *Arnt* heterozygotes. (Each knockout mouse nevertheless contains a different combination of genes derived from the 129/Sv and C57BL/6 strains.) For example, Maltepe and co-workers generated their knockout mice with R1 ES cells derived from a mating between chinchilla 129/Sv females and agouti 129/Sv-CP males, while our ES cells were derived from the 129/SvJ strain of mice with a chinchilla background. Others have reported a heterogeneity in phenotypes of particular knockout mice resulting from the use of mixed genetic backgrounds (e.g., Liu *et al.*, 1993; Dickson *et al.*, 1995). It seems unlikely that differences are the result of the region disrupted since both knockouts were generated by targeting the same restriction site in the bHLH domain. The reason for the differences among the two *Arnt* -/- mouse lines requires further study.

It has been shown that the ARNT/HIF-1 $\alpha$  dimer, under hypoxic conditions, regulates the expression of VEGF, an inducer of angiogenesis (Wood *et al.*, 1996). Furthermore,

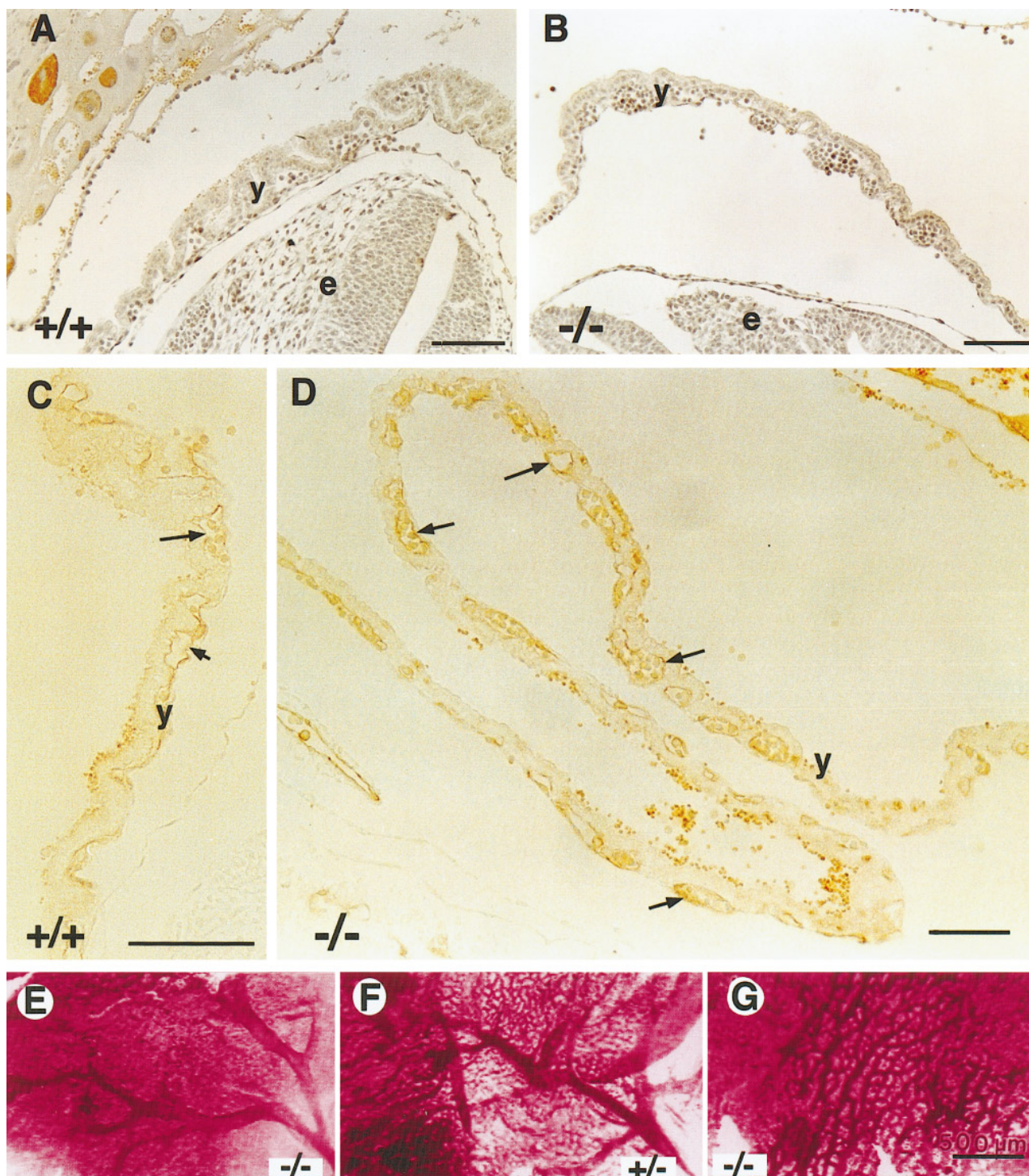


**FIG. 3.** (A–G) Yolk sac of GD 9.5 conceptus. (A,B) Both the  $+/+$  and  $-/-$  yolk sac were vascularized and, in section, the blood cells are apparent in the vessels (ARNT immunostaining with light hematoxylin counterstain). (C,D) PECAM immunostaining revealed the endothelial-cell-lined vasculature (arrows) in the yolk sac of  $+/+$  (C) and  $-/-$  (D) embryos. (E,F,G) Whole mounts of Feulgen-stained yolk sac further illustrated the extensive, well-developed GD 9.5 vascular plexus and major vessels of  $-/-$  (E,G) and  $+/-$  (F) yolk sacs. (Bar: 100  $\mu\text{m}$  in A–D and 500  $\mu\text{m}$  in E–G; y, yolk sac; e, embryo).

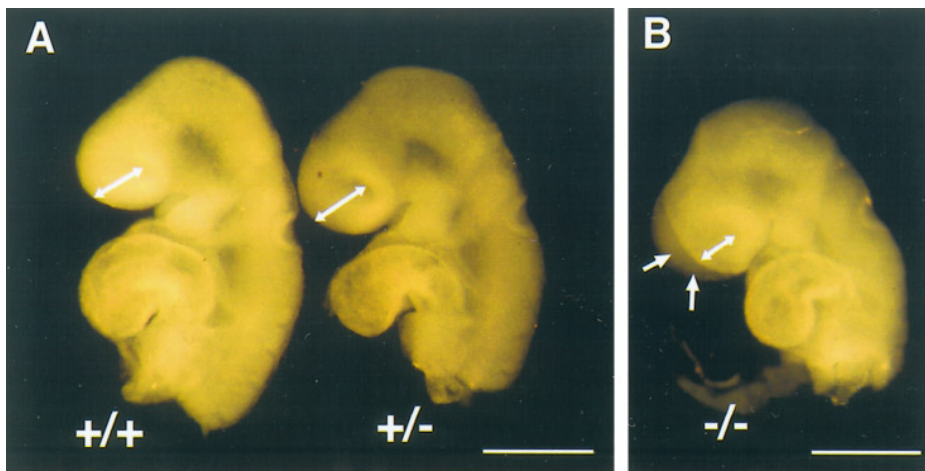


**FIG. 4.** (A,B) Embryonic phenotypic abnormalities. Embryonic development is similar between GD 9.5  $+/+$  and  $+/-$  embryos (A); however,  $-/-$  embryos exhibited neural tube defects ranging from forebrain hypoplasia to unfused head folds, or cleft face (B). The  $-/-$  embryo shown in B has unfused head folds (large arrows) and diminished distance from the anterior edge of the forebrain to posterior border of optic placode (double-headed arrows). (Bar, 100  $\mu\text{m}$ ).

VEGF  $+/-$  embryos exhibit significant defects in the vasculature of the placenta (Ferrara *et al.*, 1996). The VEGF tyrosine kinase receptors Flk-1 (VEGF-R2) and Flt-1 (VEGF-R1) are expressed in different tissues of the placenta (Breier *et al.*, 1995; Dumont *et al.*, 1995). Flk-1 is localized in the labyrinthine layer of the placenta, while Flt-1 is localized in the spongiotrophoblast layer. Flt-1 binds both VEGF and placental growth factor (Maglione *et al.*, 1991; Park *et al.*, 1994) and is essential for the organization of embryonic vasculature (Fong *et al.*, 1995). EPAS1 (HLF) also interacts with ARNT and is thought to be a regulator of vascularization. EPAS1 can activate expression of the endothelial-specific tyrosine kinase receptor Tie-2 (Tek; Tian *et al.*, 1997). The *tie-2* gene is expressed in the early embryonic vascular system, in maternal decidual vascular endothelial cells, and in extraembryonic mesoderm cells of the amnion. A *tie-2* knockout dies by GD 10.5 and has been shown to affect angiogenic processes of endothelial cells (Sato *et al.*, 1993, 1995).

We postulate that ARNT, upon dimerization with another protein (e.g., HIF-1 $\alpha$ , EPAS1), either induces the expression of an angiogenic factor (e.g., VEGF, PlGF) that acts upon receptors localized in the placenta (e.g., Flk-1, Flt-1) or induces the expression of a receptor found in the placenta (e.g., Tie-2). Loss of ARNT could thereby result in the absence of proteins required for appropriate vascular development of the placenta. The expression of such proteins may be regulated by the interaction of ARNT with a mediator of hypoxia or hypoglycemia (Maltepe *et al.*, 1997) (e.g., HIF-1 $\alpha$ , EPAS1), with the trigger possibly being generated when the yolk sac can no longer support the growing embryo. The site of such regulation in the placenta may well be the trophoblast giant cells which surround the implantation and are at the site of closest contact of maternal and embry-

onic tissues in the differentiating placenta. On GD 9–9.5, these cells increase in volume and our data show a prominent expression of ARNT which may have functional significance (Fig. 2E). The phenotypic abnormalities observed in our knockout embryos either may be a consequence of the lack of SIM1- or SIM2-ARNT dimers (or other unknown ARNT/X dimers), since both *SIM1* and *SIM2* are expressed in various tissues and organs during embryogenesis including the forebrain (Fan *et al.*, 1996; Ema *et al.*, 1996), or may be secondary to the placental defects. Further analysis of the *Arnt* knockout mice should provide insights into the molecular mechanisms regulating development of the placenta and its vasculature.

## ACKNOWLEDGMENTS

This research was funded by NIH Grant ES06439 and the UCLA Jonsson Comprehensive Cancer Center. We thank Hilde Kronenberg and Katherine Williams for technical assistance in the preparation of chimeric mice, Drs. Harvey Herschman and Srinivasa Reddy for advice and for providing plasmids, Elaine Minehart and Khurshid Muhammed for technical assistance, Judith Schmid of the Research and Support Division of the EPA for providing expert advice and statistical analysis, and Gary Held of the Reproductive Toxicology Division of the EPA for generously providing invaluable assistance in preparing the micrographs.

## REFERENCES

- Abbott, B. D., and Probst, M. R. (1995). Developmental expression of two members of a new class of transcription factors. II. Expression of aryl hydrocarbon receptor nuclear translocator in the C57BL/6N mouse embryo. *Dev. Dyn.* **204**, 144–155.



- Bradley, A. (1987). Production and analysis of chimeric mice. In "Teratocarcinomas and Embryonic Stem Cells: A Practical Approach" (E. J. Robertson, Ed.), pp. 113–151. IRL Press, Oxford/Washington, DC.
- Breier, G., Clauss, M., and Risau, W. (1995). Coordinate expression of vascular endothelial growth factor receptor-1 (Flt-1) and its ligand suggests a paracrine regulation of murine vascular development. *Dev. Dyn.* **204**, 228–239.
- Dickson, M. C., Martin, J. S., Cousins, F. M., Kulkarni, A. B., Karlsson, S., and Akhurst, R. J. (1995). Defective haematopoiesis and vasculogenesis in transforming growth factor- $\beta$ 1 knock out mice. *Development* **121**, 1845–1854.
- Dumont, D., Fong, G-H., Puri, M. C., Gradwohl, G., Alitalo, K., and Breitman, M. L. (1995). Vascularization of the mouse embryo: A study of *flk-1*, *tek*, *tie*, and vascular endothelial growth factor expression during development. *Dev. Dyn.* **203**, 80–92.
- Ema, M., Morita, M., Ikawa, S., Tanaka, M., Matsuda, Y., Gotoh, O., Saijoh, Y., Fujii, H., Hamada, H., Kikuchi, Y., and Fujii-Kuriyama, Y. (1996). Two new members of the murine *Sim* gene family are transcriptional repressors and show different expression patterns during mouse embryogenesis. *Mol. Cell. Biol.* **16**, 5865–5875.
- Ema, M., Taya, S., Yokotani, N., Sogawa, K., Matsuda, Y., and Fujii-Kuriyama, Y. (1997). A novel bHLH-PAS factor with close sequence similarity to hypoxia-inducible factor 1 $\alpha$  regulates the VEGF expression and is potentially involved in lung and vascular development. *Proc. Natl. Acad. Sci. USA* **94**, 4273–4278.
- Fan, C. M., Kuwana, E., Bulfone, A., Fletcher, C. F., Copeland, N. G., Jenkins, N. A., Crews, S., Martinez, S., Puellas, L., Rubenstein, J. L., and Tessier-Lavigne, M. (1996). Expression patterns of two murine homologs of *Drosophila* single-minded suggest possible roles in embryonic patterning and in the pathogenesis of Down syndrome. *Mol. Cell. Neurosci.* **7**, 1–16.
- Ferrara, N., Carver-Moore, K., Chen, H., Dowd, M., Lu, L., O'Shea, K. S., Powell-Braxton, L., Hillan, K. J., and Moore, M. W. (1996). Heterozygous embryonic lethality induced by targeted inactivation of the *VEGF* gene. *Nature* **380**, 439–442.
- Fong, G-H., Reascend, J., Gertsenstein, M., and Breitman, M. L. (1995). Role of the Flt-1 receptor tyrosine kinase in regulating the assembly of vascular endothelium. *Nature* **376**, 66–70.
- Fukunaga, B. N., Probst, M. R., Reisz-Porszasz, S., and Hankinson, O. (1995). Identification of functional domains of the aryl hydrocarbon receptor. *J. Biol. Chem.* **270**, 29270–29278.
- Guillemot, F., Nagy, A., Auerbach, A., Rossant, J., and Joyner, A. L. (1994). Essential role of *Mash-2* in extraembryonic development. *Nature* **371**, 333–336.
- Gurtner, G. C., Davis, V., Li, H., McCoy, M. J., Sharpe, A., and Cybulsky, M. I. (1995). Targeted disruption of the murine *VCAM1* gene: Essential role of the VCAM-1 in chorioallantoic fusion and placentation. *Genes Dev.* **9**, 1–14.
- Hankinson, O. (1995). The aryl hydrocarbon receptor complex. *Annu. Rev. Pharmacol. Toxicol.* **35**, 307–340.
- Liu, J. P., Baker, J., Perkins, A. S., Robertson, E. J., and Efstradiadis, A. (1993). Mice carrying null mutations of the genes encoding insulin-like growth factor I (Igf-1) and type 1 IGF receptor (Igf1r). *Cell* **75**, 59–72.
- Maglione, D., Guerriero, V., Viglietto, G., Delli-Bovi, P., and Persico, M. G. (1991). Isolation of a human placenta cDNA coding for a protein related to the vascular permeability factor. *Proc. Natl. Acad. Sci. USA* **88**, 9267–9271.
- Maltepe, E., Schmidt, J. V., Baunoch, D., Bradfield, C. A., and Simon, M. C. (1997). Abnormal angiogenesis and response to glucose and oxygen deprivation in mice lacking the protein ARNT. *Nature* **386**, 403–407.
- Mansour, S. L., Thomas, K. R., and Capecchi, M. R. (1988). Disruption of the proto-oncogene *int-2* in mouse embryo-derived stem cells: A general strategy for targeting mutations to non-selectable genes. *Nature* **336**, 348–352.
- Park, J. E., Chen, H. H., Winer, J., Houck, K. A., and Ferrara, N. (1994). Placenta growth factor. Potentiation of vascular endothelial growth factor bioactivity, in vitro and in vivo, and high affinity binding to Flt-1 but not Flk-1/KDR. *J. Biol. Chem.* **269**, 25646–25654.
- Probst, M. R., Fan, C. M., Tessier-Lavigne, M., and Hankinson, O. (1997). Two murine homologs of the *Drosophila* single-minded protein that interact with the mouse aryl hydrocarbon receptor nuclear translocator protein. *J. Biol. Chem.* **272**, 4451–4457.
- Probst, M. R., Reisz-Porszasz, S., Agbunag, R. V., Ong, M. S., and Hankinson, O. (1993). Role of the aryl hydrocarbon receptor nuclear translocator protein in aryl hydrocarbon (dioxin) receptor action. *Mol. Pharmacol.* **44**, 511–518.
- Reisz-Porszasz, S., Probst, M. R., Fukunaga, B. N., and Hankinson, O. (1994). Identification of functional domains of the aryl hydrocarbon receptor nuclear translocator protein (ARNT). *Mol. Cell. Biol.* **14**, 6075–6086.
- Sato, T. N., Qin, Y., Kozak, C. A., and Audus, K. L. (1993). *Tie-1* and *tie-2* define another class of putative receptor tyrosine kinase genes expressed in early embryonic vascular system. *Proc. Natl. Acad. Sci. USA* **90**, 9355–9358.
- Sato, T. N., Tozawa, Y., Deutsch, U., Wolburg-Buchholz, K., Fujiwara, Y., Gendron-Maguire, M., Gridley, T., Wolburg, H., Risau, W., and Qin, Y. (1995). Distinct roles of the receptor tyrosine kinase *Tie-1* and *Tie-2* in blood vessel formation. *Nature* **376**, 70–74.
- Thomas, K. R., and Capecchi, M. R. (1987). Site-directed mutagenesis by gene targeting in mouse embryo-derived stem cells. *Cell* **51**, 503–512.
- Tian, H., McKnight, S. L., and Russell, D. W. (1997). Endothelial PAS domain protein 1 (EPAS1), a transcription factor selectively expressed in endothelial cells. *Genes Dev.* **11**, 72–82.
- Wang, G. L., and Semenza, G. L. (1995). Purification and characterization of hypoxia-inducible factor 1. *J. Biol. Chem.* **270**, 1230–1237.
- Wood, S. M., Gleadle, J. M., Pugh, C. W., Hankinson, O., and Ratcliffe, P. J. (1996). The role of the aryl hydrocarbon receptor nuclear translocator (ARNT) in hypoxic induction of gene expression. Studies in ARNT-deficient cells. *J. Biol. Chem.* **271**, 15117–15123.

Received for publication July 29, 1997

Accepted September 22, 1997